

Long chain branching in low density polyethylene: 2. Rheological behaviour of the polymers

Daniele Romanini and Aurelio Savadori

Montedison Centro Ricerche, Ferrara, Italy

and Giuseppe Gianotti

Montedison Ist. Ric. 'G. Donegani', Novara, Italy

(Received 6 March 1979)

Investigations have been carried out by different methods on the rheological properties, both shear and tensile, of some unfractionated samples of low density polyethylene, the molecular characteristics and long chain branching content being known. From the comparison with analogous linear polyethylenes it clearly appears that correlations exist between the long chain branching content and the main viscous and elastic parameters of the melt. The results obtained illustrate the possibility of reaching a preliminary evaluation of the *LCB* degree in the integral polyethylene samples by simple rheological measurements.

INTRODUCTION

Low-density polyethylenes (LDPE) obtained by high pressure processes are generally characterized by simple parameters, such as density, melt flow rate, intrinsic viscosity. However, these polymers may exhibit no difference in such parameters, but yet they may show markedly different applicative properties, due to their different molecular structures.

A number of investigations have been carried out by several authors in order to clarify the relationships existing between polyethylene rheological behaviour in the molten state and its molecular structure. The dependence of the flow properties of the linear polymers on the average molecular weight is fairly clear¹⁻⁴; the influence of long chain branchings (*LCB*) in LDPE on the rheological behaviour particularly with regard to elastic effects, is less evident⁵⁻¹⁶. The aim of this work is to establish the correlations existing between molecular parameters and rheological behaviour in the molten state of some LDPE samples, the *LCB* content of which is known from the first part of this study¹⁷ and from previous work¹⁸. Here, the investigation is limited to integral samples. The study will be subsequently extended to mono-disperse fractions of the same products.

EXPERIMENTAL

Materials

The examined samples consisted of low-density polyethylenes of Montedison production obtained by high-pressure processes using different methods of synthesis. As references, a sample of linear polyethylene (No. 1475 National Bureau of Standards) and three substantially linear high-density polyethylenes (HDPE) with a higher molecular weight were considered.

* Presented in part at the Joint Conference on 'The rheology of associating, structured and biological systems', Amsterdam, April 18-20, 1979.

Table 1 outlines the main chemico-physical characteristics of the polymers used; samples 1-5 were obtained in a tubular reactor under particular conditions of synthesis, whilst samples 6-14 were produced by a vessel reactor consisting of a autoclave divided into conveniently arranged multiple reaction chambers.

The intrinsic viscosity, $[\eta]$, was measured in orthodichlorobenzene at 135°C, by modified Desreux-Bischoff viscometers¹⁹. The average weight molecular weight \bar{M}_w was determined by light scattering, Sofica type, in α -chloronaphthalene at 125°C. Density was measured at 23°C, according to the ASTM-D-1505/68 method. The melt flow rate (*MFR*) was evaluated according to the ASTM-D-1238/73 method, condition *E* procedure B. The β factor is the dimensional polydispersity expressed as the ratio \bar{A}_w/\bar{A}_n , determined by g.p.c. in orthodichlorobenzene at 135°C¹⁷.

Constant pressure capillary rheometer

Use was made of the rheometer mod. 6540 of Ceast (Turin) which detects the time that is required to extrude, through a capillary, a known volume of polymer under constant pressure. Using this capillary rheometer *MFR* runs were carried out at 190°C and the average die swell *B* (expressed as the ratio of the diameter of the extruded polymer to that of the spinneret) was determined both before and after 10 min annealing in silicon oil respectively at 130°C for LDPE and 150°C for HDPE.

The capillary used was 2.095 mm in diameter, 8 mm long and had an inlet angle of 180°; the shear stress constantly applied was 19560 Nm⁻² and temperature 190°C.

Constant-rate capillary rheometer

Use was made of a viscosimeter of the Merz-Colwell (*MCR*) type of Instron²⁰ where the material is pushed through a capillary at a constant extrusion rate; the applied shear stress was measured by a load cell situated at the top of the pushing piston. The shear stress τ_w and the apparent shear

Table 1 Specifications of polyethylenes

No.	Sample	Synthesis process	Density 23°C (g cm ⁻³)	MFR (g 10 min ⁻¹)	[η] _{ODCB} ^{135°C} (dl g ⁻¹)	M_w , 10 ⁻³	β
1	T-1	Tubular	0.9176	2.14	0.88	280	5.4
2	T-2	Tubular	0.9172	1.57	0.88	360	5.7
3	T-3	Tubular	0.9176	0.24	1.04	550	5.7
4	TM-1	Modified tubular	0.9205	3.12	0.78	120	4.9
5	TM-2	Modified tubular	0.9234	2.13	0.83	135	4.1
6	V-1	Vessel	0.9128	84.0	0.66	210	6.6
7	V-2	Vessel	0.9144	22.4	0.83	340	8.8
8	V-3	Vessel	0.9156	6.58	0.96	420	9.6
9	V-4	Vessel	0.9176	1.19	1.08	690	9.4
10	VM-1	Modified vessel	0.9198	1.75	0.91	140	4.5
11	VM-2	Modified vessel	0.9204	1.69	0.89	185	5.5
12	VM-3	Modified vessel	0.9211	0.25	1.12	275	4.7
13	VM-4	Modified vessel	0.9207	0.24	1.16	330	5.8
14	VM-5	Modified vessel	0.9217	0.24	1.14	600	6.6
15	1475 NBS		0.9780	15.1	1.00	52	3.0
16	HDPE-1		0.9500	0.98	1.72	110	5.3
17	HDPE-2		0.9445	0.21	1.95	140	8.0
18	HDPE-3		0.9440	0.04	2.40	220	9.1

rate $\dot{\gamma}_a$ were calculated at the capillary wall by the known relationships⁷

$$\tau_w = \frac{PR}{2L} \quad (1)$$

$$\dot{\gamma}_a = \frac{4Q}{\pi R^3} \quad (2)$$

where P is the applied pressure (N m⁻²), Q the volumetric flow rate (m³ s⁻¹), R, L the radius and respectively the length of the capillary (m). The apparent viscosity η_a is given by:

$$\eta_a = \frac{\tau_w}{\dot{\gamma}_a} \quad (3)$$

Using such a rheometer it was possible to determine the flow curves of the polyethylenes under examination at different temperatures as well as the activation energies of the viscous flow, by the use of just one capillary with inlet angle of 90°, 1.26 mm i.d., 51 mm long ($L/D = 40.5$), thus covering the shear rate range from 3 to 3000 s⁻¹.

Owing to the type of capillary adopted, corrections for the inlet effects were neglected²¹; the Rabinowitsch correction²² was not calculated from flow curves, hence the reported curves were non-corrected²³⁻²⁴. Temperatures were kept constant at $\pm 0.5^\circ\text{C}$.

Melt tension tester (MTT)

This rheometer, type II of Toyo Seiki Seisakusho Ltd.²⁵ allowed the determination of the apparent melt viscosity at different shear rates and of the tensile properties of the extruded polymer, which was stretched, at a variable rate, by a drawing roll system. The scheme is shown in Figure 1.

In order to perform tensile measurements, the polymer was extruded at constant rate and the monofilament formed at the capillary outlet was passed through a pulley system, then drawn by two counter-rotating rolls, the tangential rate of which could be continuously varied from 0 to 350 m min⁻¹. A force detector connected to the first pulley situated 30 cm

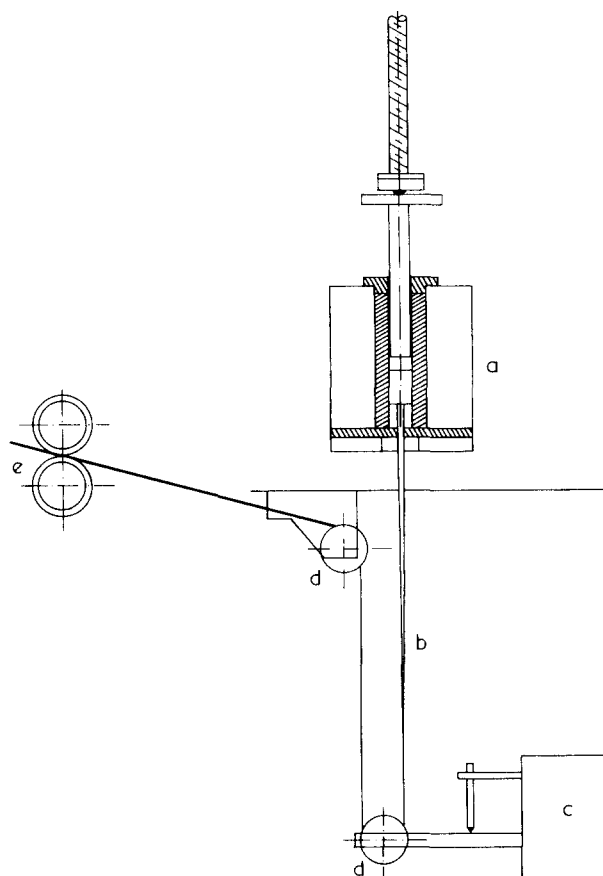


Figure 1 Schematic diagram of 'melt tension tester' (a) extrusion part; (b) monofilament of polymer; (c) strain gauge; (d) pulley; (e) drawing roll

from the capillary measured the melt strength of the monofilament at the different drawing rates.

With MTT, at a constant extrusion rate (3×10^{-3} m s⁻¹), the melt strength and the breakage stretch ratio of the monofilament extruded at $180^\circ\text{C} \pm 0.2^\circ\text{C}$ were determined, by the use of a capillary, 1 mm i.d., 8 mm long and inlet angle of 180° . The stretching run was carried out under non-iso-

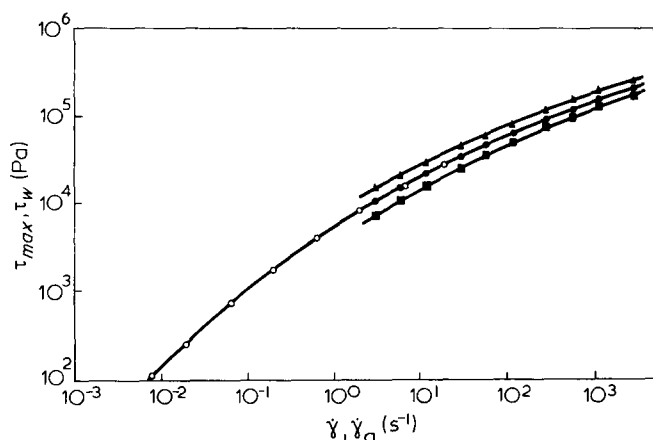


Figure 2 Typical flow curve, shear stress τ versus shear rate $\dot{\gamma}$, of the sample no 1 by means of *WRG* (○, 180°C) and *MCR* (▲, 160°C; ●, 180°C; ■, 200°C)

thermic conditions in an air conditioned environment at 23°C. The breakage stretch ratio of polyethylene No. 15 (1475 NBS) was not determined because its flowability is so high that it can be stretched beyond the maximum limit of the apparatus.

Weissenberg rheogoniometer (WRG)

Use was made of model R-18 of Sangamo Control Ltd.²⁰, in this rotational viscosimeter, the molten material undergoes deformation between the flat surface and the rotating cone; its cone angle has been chosen so as to obtain, in the whole fluid mass, almost constant shear stress and shear rate, in flow steady state.

The shear rate is given by:

$$\dot{\gamma} = \frac{\Omega}{\alpha} \tag{4}$$

where Ω is the angular velocity of the rotating cone and α the angle between a cone generator and the plane.

The shear stress in all points of the fluid is given by:

$$\tau = \frac{3M}{2\pi r^3} \tag{5}$$

where r is the radius of the plate and of the cone basis, M is the torque transmitted from the material to the upper plate.

For the apparent viscosity one obtains:

$$\eta_a = \frac{3M\alpha}{2\pi r^3 \Omega} \tag{6}$$

A fundamental peculiarity of the rheogoniometer, in view of the aims of our work, is the possibility of investigating the range of low shear rates (of the order of 10^{-3} s^{-1}), which is the most affected by the structural-molecular properties of the polymers.

The low shear rate flow curves and the relaxation times of shear stress at $180^\circ\text{C} \pm 1^\circ$ have been determined on the samples under examination, by the use of a cone and plate with diameter of 25 mm and cone angle of about 1° .

The elastic constant of the torsional spring was $9.43 \times 10^{-5} \text{ Nm}$ for $1 \mu\text{m}$ transducer shift. The values of η_a were

calculated by using the highest shear stress, τ_{max} , from stress-strain curves for each shear rate examined; in this way a good agreement was obtained between the flow curves by *WRG* and the non-corrected ones measured by *MCR*²⁶.

The relaxation curves of shear stresses were measured by stopping strain when shear stress had reached the maximum of the stress-strain curve, and then by recording the decrease in stress with time for each shear rate examined. The relaxation curves obtained under such operating conditions have a relative comparative value in that, as a rheogoniometer modified according to Meissner²⁷ was not available, it should have been more correct to use a very stiff torsional spring (although this would have been to the detriment of viscosity measurements) and a higher-angle cone. However, to preserve uniform operating conditions, this was not done for measurements on monodispersed fractions, available in very small amounts²⁸.

RESULTS AND DISCUSSION

Flow curves

By means of the apparatus previously described, evaluations were carried out on the rheological behaviour of the samples under examination, in order to discover possible differences between linear and branched polyethylenes. The flow curves are expressed as shear stress vs shear rate; the results obtained by the rheogoniometer are indicated by τ_{max} and those obtained by the capillary rheometer by τ_w . The good agreement between the *WRG* and *MCR* data is shown in the typical flow curve of Figure 2. A significant comparison among polyethylenes with a different *LCB* degree, but with a fairly close weight average molecular weight is shown in Figure 3, where the curve of sample 7, the most branched one, is much lower than that of sample 2 and even more in respect of linear sample 17, in spite of its lower molecular weight.

The limiting Newtonian viscosity η_o was determined for all samples at 180°C (Table 2); this was obtained experimentally for most samples, whilst for some others (HDPE-2 and HDPE-3) it was calculated from the activation energy, by assuming it to be constant to very low values of shear stress, and by extrapolation²⁰.

By plotting the shear stress τ vs the reduced variable $\eta_o \dot{\gamma}$, which normalizes the effect of temperature on the

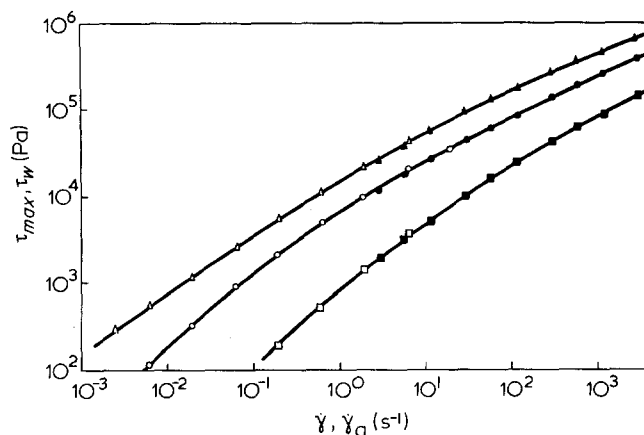
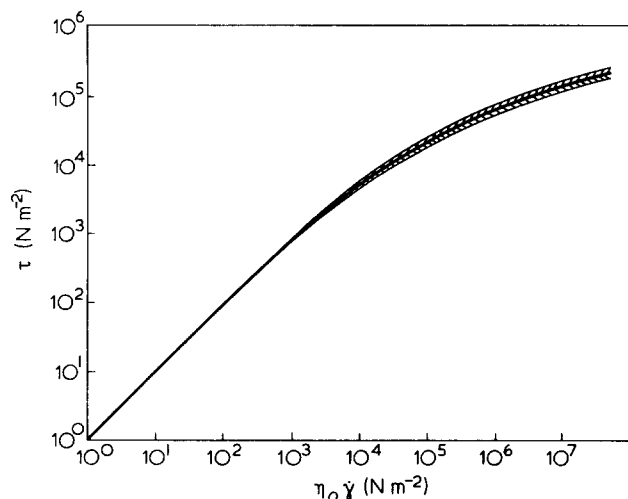


Figure 3 Shear stress τ versus shear rate $\dot{\gamma}$ at 180°C of the samples no. 7 (□, *WRG*; ■, *MCR*), no 2 (○, *WRG*; ●, *MCR*), and no 17 (△, *WRG*; ▲, *MCR*)

Table 2 Rheological parameters from the flow curves of samples examined

Sample No.	$\eta_o 10^{-3}$ 180°C (Pa.s)	$\dot{\gamma}_o$ 180°C (s ⁻¹)	E_τ (Kcal mol ⁻¹)	λ_o 180°C (s)
1	13	4×10^{-2}	12.4 → 9	7
2	18	3×10^{-2}	10.4	9
3	130	2×10^{-3}	—	80
4	8.5	6×10^{-2}	—	3.4
5	12	5×10^{-2}	10.2 → 8.2	4
6	0.16	2×10^0	8.7	—
7	0.95	1×10^0	8.8	0.6
8	4	1.2×10^{-1}	8.8	3.5
9	18	2×10^{-2}	10	13
10	10	1.5×10^{-1}	12.2 → 8.6	3.5
11	16	3×10^{-2}	—	6
12	110	5×10^{-3}	—	55
13	130	5×10^{-3}	9.4	70
14	80	6×10^{-3}	—	40
15	0.78	2×10^0	—	0.22
16	22	2×10^{-2}	6.4	9
17	160	1×10^{-3}	6.2	150
18	~1200	~ 1×10^{-4}	5.8	~1100


Figure 4 Shear stress τ versus $\eta_o \dot{\gamma}$ product for all LDPE examined by *WRG* and *MCR* rheometers at different temperatures: \square , samples by vessel process and \boxplus , samples by tubular process

melt viscosity, a curve has been drawn representing the flow properties of low-density polyethylenes (*Figure 4*); all experimental values obtained on LDPE by the above techniques are situated in the hatched area.

As may be seen, dispersion increases in the high shear region, obviously due to the different pseudo-plasticity of the samples, although it does not exceed $\pm 20\%$ of the average of τ at a fixed $\eta_o \dot{\gamma}$. The vessel products are situated in the upper part of the band, while the tubular ones are in the lower part. That means that the rheological behaviour at high shear rates of the polyethylenes obtained by the tubular process is markedly pseudo-plastic. This is probably due to the lower long branching content of these polymers, in comparison with the corresponding vessel ones.

The average behaviour may be represented by the following relationship, which is valid in a $\eta_o \dot{\gamma}$ range between 10^2 and 10^8 N m⁻²:

$$\log \tau = -0.275 + 1.283 \log(\eta_o \dot{\gamma}) - 0.072 [\log(\eta_o \dot{\gamma})]^2 \quad (7)$$

which allows one to single out, to a good approximation, the full flow curve of a low-density polyethylene from the shear stress measurement within a narrow range of shear rates. In the $10^0 < \eta_o \dot{\gamma} < 10^2$ region, all experimental points found by the authors fell on the unitary slope straight line.

Limiting Newtonian viscosity

From the flow curves at 180°C, the Newtonian viscosity η_o and the shear rate $\dot{\gamma}_o$, at which viscosity underwent a 10% decrease over the value of η_o at that temperature (*Table 2*) were determined; such a shear rate has been assumed to be the limit where the rheological behaviour of the material stops being Newtonian.

Figure 5 plots the log-log values of η_o at 180°C, as a function of $\dot{\gamma}_o$, multiplied by polydispersity β , on which it depends^{4,30}; all examined polyethylenes, the linear ones included, fall on the straight line represented by the equation:

$$\log \eta_o = -0.77 \log(\beta \dot{\gamma}_o) + 3.68 \quad (8)$$

which, for the experimental values obtained, is satisfied by a correlation coefficient of 0.99.

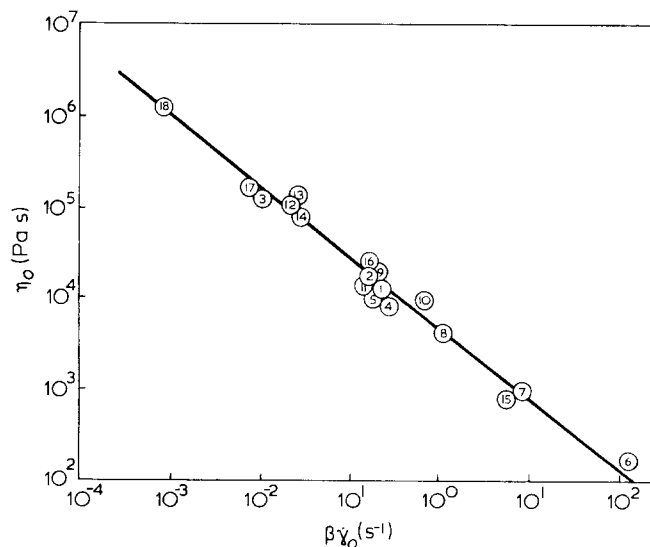
Since the variability range of β is limited in respect of that of $\dot{\gamma}_o$, and exclusively contributes to improve the correlation coefficient of the dependence equation, it may be assumed that the existing relationship between η_o and $\dot{\gamma}_o$ is

$$\dot{\gamma}_o = \text{const. } \eta_o^{-a} \quad (9)$$

This suggests that the limiting shear rate $\dot{\gamma}_o$ is governed by the same molecular parameters influencing the Newtonian viscosity η_o . Hence, on the basis of equation (9), at a given temperature the decrease in viscosity by the effect of *LCB* involves an increase in $\dot{\gamma}_o$, connected with the values of the constant and of exponent a ; for a particular case at 180°C:

$$\dot{\gamma}_o = 1.83 \times 10^5 \eta_o^{-1.56} \quad (10)$$

where an average $\beta = 6.5$ is at the assumed temperature of 180°C. Obviously, the relationship becomes more approximate as the variability range of β becomes narrower.


Figure 5 Melt Newtonian viscosity η_o versus $\beta \dot{\gamma}_o$ product at 180°C for all samples examined. Each sample is numbered as appears in *Table 1*

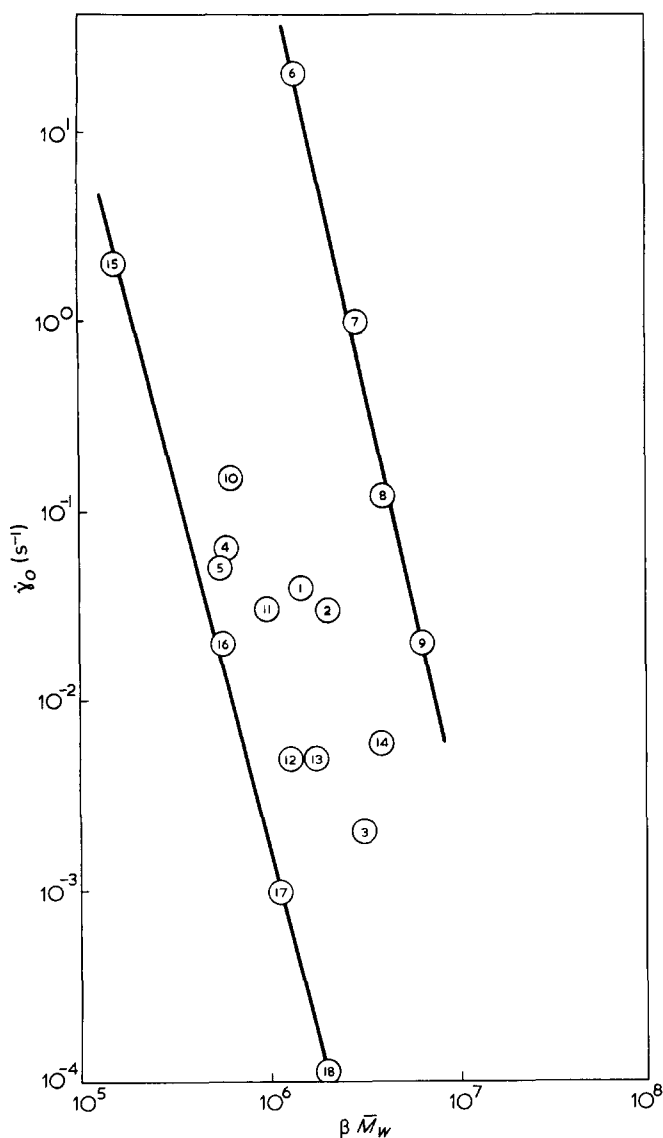


Figure 6 Limiting Newtonian shear rate $\dot{\gamma}_0$ at 180°C versus molecular parameter $\beta \bar{M}_w$ for samples employed

Such behaviour is better illustrated in Figure 6, where the shear rate $\dot{\gamma}_0$ is reported as a function of the molecular parameter $\beta \bar{M}_w$; actually it may be noticed that a high long branching content shifts the limiting Newtonian shear rate toward much higher values, the molecular weight and dimensional polydispersity being the same.

Figures 7 and 8 show the correlations between Newtonian viscosities η_0 and respectively the molecular weight \bar{M}_w , and the molecular weight corrected for polydispersity $\beta \bar{M}_w$. They both clearly show how, the molecular weight being the same, the Newtonian viscosity markedly decreases on increasing the LCB content; polydispersity causes a decrease in the slope of the straight lines drawn for linear and vessel polyethylenes, but leaves the viscosity η_0 fall due to branchings substantially unaltered.

Considering the four linear polymers investigated, the relationships shown in Figures 7 and 8 respectively, may be written:

$$\log \eta_0 (180^\circ\text{C}) = 5.16 \log \bar{M}_w - 21.48 \quad (11)$$

(corr. coeff. 0.995)

$$\log \eta_0 (180^\circ\text{C}) = 2.84 \log(\beta \bar{M}_w) - 11.95 \quad (12)$$

(corr. coeff. 0.997)

Such results suggest that, in the Newtonian region, the flow behaviour depends more extensively on the physical and interaction parameters among macromolecules than on the molecular properties. At most, it might be assumed that the Newtonian viscosity η_0 is directly connected, like the viscosity in solution, with the statistical dimensions of the bundle associated with the macromolecule³¹⁻³³, which decrease as the LCB content increases.

Linear and branched polyethylenes may have the same η_0 , though exhibiting a very different weight average molecular weight. An investigation may be adequately developed only on mono-dispersed fractions in order to correlate directly the molecular dimensions to the Newtonian viscosity of linear and branched samples. There are, however, great experimental difficulties involved in an approach of this type.

Activation energy of the viscous flow

By applying the known Arrhenius equation to the flow curves determined by the Instron rheometer at different temperatures (160, 180, 200, 220°C), the activation energies at different shear stress were calculated.

Contrary to what was found for linear polyethylenes, which exhibit a constant activation energy close to 6 kcal mol⁻¹, LDPE have a higher activation energy E_T that, in some cases, decreases on increasing the shear stress τ . Table 2 show the data obtained in a shear stress range from 5 ×

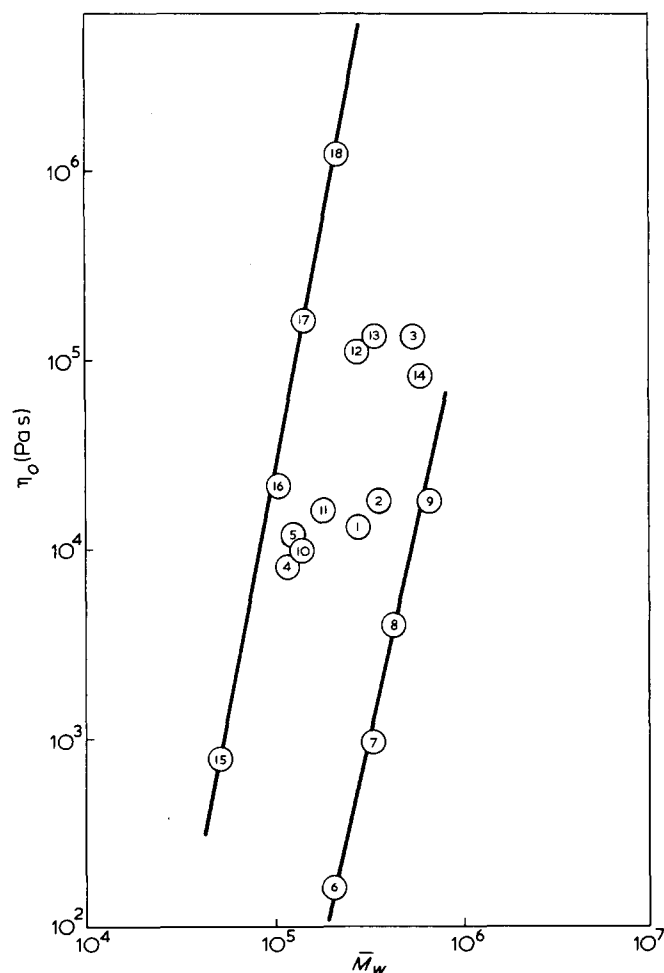


Figure 7 Melt Newtonian viscosity η_0 at 180°C versus weight average molecular weight \bar{M}_w of samples examined

product $\beta\eta_0$, as shown in Figure 9; its regression straight line has the equation:

$$\log \lambda_0 = 1.04 \log (\beta\eta_0) - 4.25 \quad (\text{corr. coeff. } 0.997) \quad (14)$$

Both (13) and (14) were calculated by excluding the values of sample 18, since its λ_0 was only approximately evaluated. The flowability of sample 6 being very high, it was not possible to detect its relaxation times.

Such results clearly indicate that the limiting relaxation time λ_0 is substantially governed by the same molecular parameters that η_0 depends on, except, perhaps, a greater sensitivity of λ_0 toward the dimensional polydispersity β , as might be suggested by the almost unitary slope of the straight line equation¹⁴.

Figure 10 plots λ_0 at 180°C vs the product $\beta\bar{M}_w$, which exhibits a similar behaviour to that of η_0 of Figure 8; it is clearly apparent that the relaxation time of tangential stress in the molten state increases with increased molecular weight and markedly decreases with long branching³⁷.

As for the linear polyethylene samples investigated, the dependences at 180°C of λ_0 respectively on \bar{M}_w and $\beta\bar{M}_w$, may be written:

$$\log \lambda_0 = 6.06 \log \bar{M}_w - 29.3 \quad (\text{corr. coeff. } 0.988) \quad (15)$$

$$\log \lambda_0 = 3.36 \log (\beta\bar{M}_w) - 18.2 \quad (\text{corr. coeff. } 0.996) \quad (16)$$

The slopes of the representative straight lines are slightly higher in respect to those of equations (11) and (12); this fact may confirm our suspicion of a greater sensitivity of the relaxation time λ_0 from the molecular weight \bar{M}_w and from the polydispersity β , in respect of the Newtonian viscosity η_0 .

From the viscoelastic models, the significance of the characteristic relaxation time as a ratio between the viscous constant on an elastic modulus permits the limiting shear

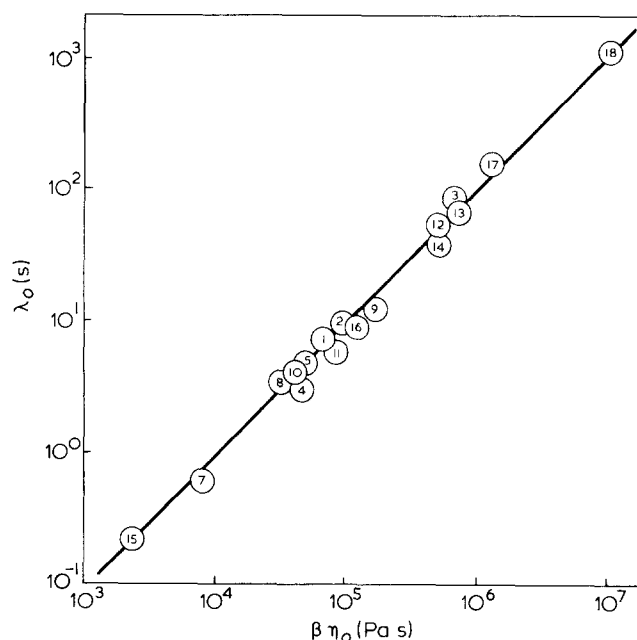


Figure 9 Limiting relaxation time λ_0 versus $\beta\eta_0$ product for samples tested at 180°C by means of WRG

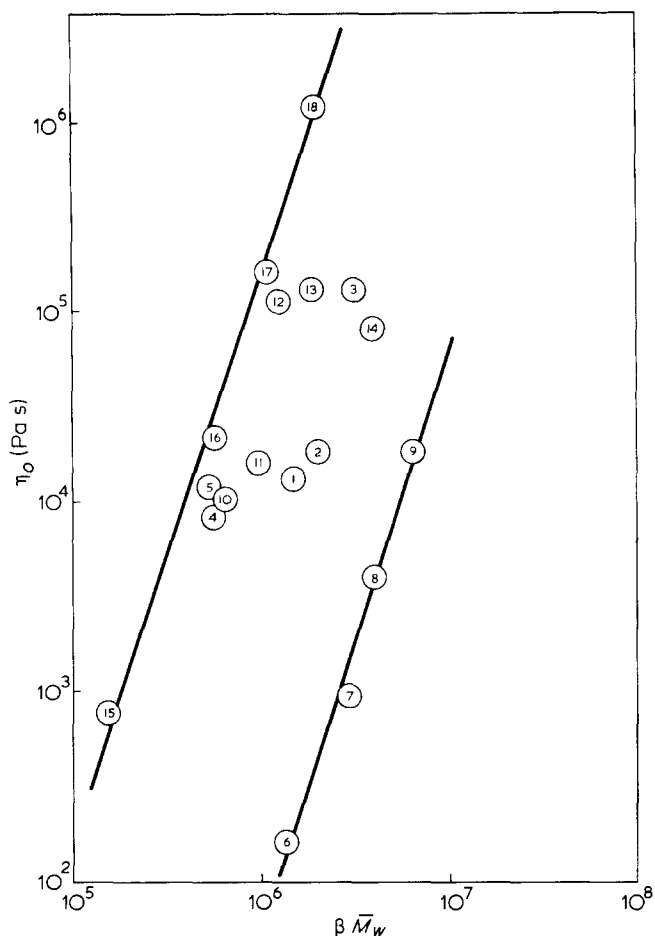


Figure 8 Melt Newtonian viscosity η_0 at 180°C versus $\beta\bar{M}_w$ product for all polyethylenes used

10^3 to $5 \times 10^5 \text{ N m}^{-2}$; the values of E_τ were calculated at the extremes of this stress range.

Several authors agree upon attributing the irregular behaviour of energy E_τ to branchings; in particular, its increase in respect of linear polyethylenes seems to be due to the interaction of long branchings with the other polymeric chains^{1,34}; E_τ should be the higher the wider the interaction range of LCB and the lower the mobility of macromolecules^{35,36}.

Relaxation times in the molten state

Relaxation measurements carried out by WRG have given the time λ required by tangential stress τ to relax to e^{-1} of its initial value, which, in our case, was the maximum of the stress-strain curve.

Such a relaxation time λ was measured for different shear rate values; by log-log plotting $\lambda = f(\dot{\gamma})$, a set of curves similar to $\eta = f(\dot{\gamma})$ were obtained.

In this way, a constant limiting relaxation time λ_0 could be determined by extrapolating the λ values at very low $\dot{\gamma}$, in analogy with the procedure adopted to obtain the Newtonian viscosity η_0 .

A preliminary interesting result has been obtained by correlating the λ_0 values with η_0 in log-log, at 180°C; a straight-line equation is obtained:

$$\log \lambda_0 = 1.07 \log \eta_0 - 3.59 \quad (\text{corr. coeff. } 0.98) \quad (13)$$

A better dependence is found by correlating λ_0 with the

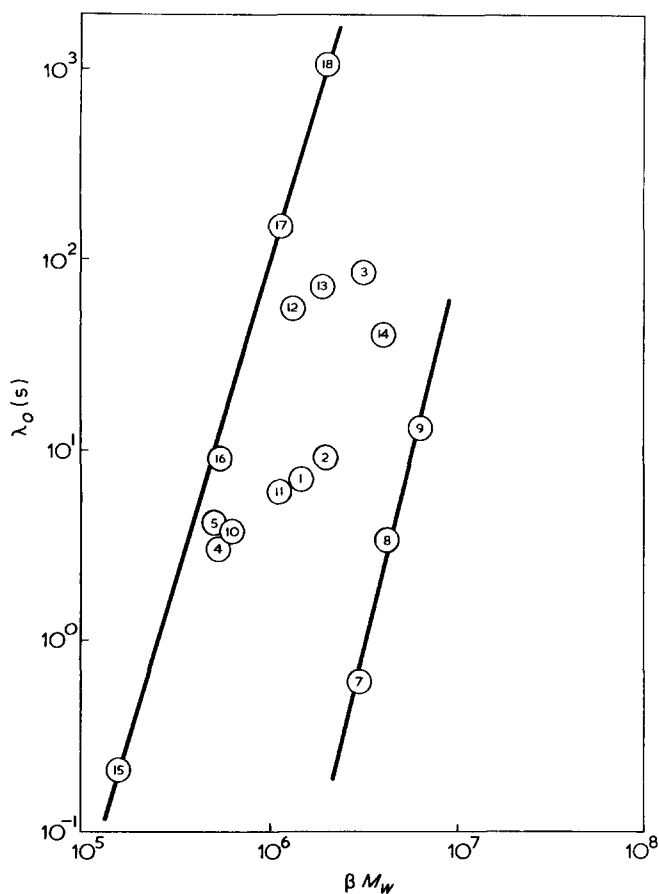


Figure 10 Limiting relaxation time λ_0 at 180°C versus $\beta\bar{M}_w$ product of polyethylenes examined

modulus, G_0 , to be obtained from the relation:

$$G_0 = \frac{\eta_0}{\lambda_0} \quad (17)$$

Since the correlation between λ_0 and η_0 is almost linear, as is apparent from equation (13), one may expect the melt limiting shear modulus G_0 to change a little with the molecular weight.

In fact, all samples examined here have G_0 values within 1.1×10^3 and 3.5×10^3 Pa; these are the extreme values of the linear polyethylenes, while the LDPE samples are in an even more narrow range.

Extruded polymer swell data

The swelling ratio B obtained by constant pressure capillary rheometer is shown in Table 3. It appears that the elastic deformation recovery by the effect of annealing averagely equals 5–6% for low-density products, and 16% for the high-density ones

Such a difference may be partly attributed to the lower time required by HDPE to reach crystallization temperature once extruded from the capillary, and partly to the long branchings present in LDPE; actually, as previously seen, these cause a decrease in the relaxation times of stresses, and therefore favour deformation recovery.

As for sample 18 (HDPE-3), due to its high viscosity, no significant swell measurements under the operating conditions adopted for the other products could be done.

Figure 11 plots the die swell B_a after annealing vs. the molecular parameter $\beta\bar{M}_w$. In spite of the discrepancies

found in literature concerning the effect of \bar{M}_w and of polydispersity $\beta^{38,39}$, we have found that the extruded polymer swell increases with the increase of these parameters; instead, $\beta\bar{M}_w$ being the same, long branchings cause a swell decrease. Consequently, the molecular weight and polydispersity being the same, the elastic deformation of LCB polyethylene, which may be recovered in the molten state, is lower than that of the corresponding linear one, under the same applied shear stress¹². This finding may be explained by the fact that the molecular size decrease due to LCB leads, under the same applied stress, to a lower deformability.

This conclusion is proved by Figure 12, which shows the dependence of the B_a/MFR ratio (between the swell after annealing and melt flow rate at the same temperature and with an identical shear stress) on molecular weight \bar{M}_w . In fact, such a ratio may be assimilated to the balance between the elastic and viscous component of the material. The molecular weight being the same, the long branching causes a shift of this ratio toward lower values, correspond-

Table 3 Die swell of the extruded polymers at 190°C

Sample No.	B	B_a (after annealing)	Increasing %
1	1.46	1.54	+5.5
2	1.53	1.63	+6.5
3	1.46	1.57	+7.5
4	1.39	1.42	+2.2
5	1.36	1.42	+4.4
6	1.32	1.41	+6.8
7	1.62	1.71	+5.5
8	1.72	1.83	+6.4
9	1.66	1.80	+8.4
10	1.43	1.51	+5.6
11	1.46	1.53	+4.8
12	1.42	1.50	+5.6
13	1.43	1.51	+5.6
14	1.60	1.69	+5.6
15	1.35	1.57	+16.3
16	1.48	1.75	+18.2
17	1.66	1.90	+14.5
18	—	—	—

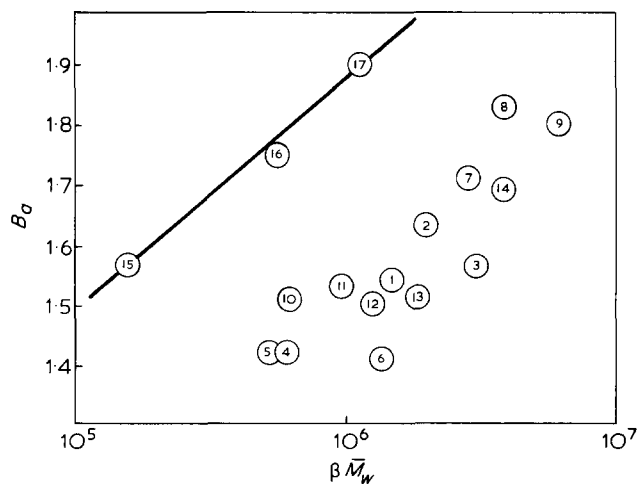


Figure 11 Die swell after annealing B_a versus $\beta\bar{M}_w$ product of the samples extruded at 190°C by means of constant pressure rheometer

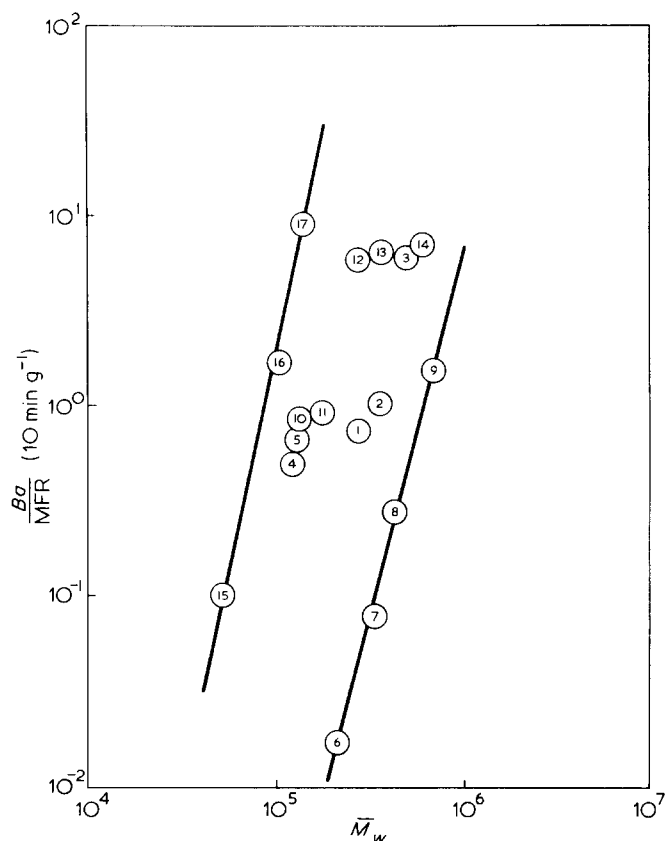


Figure 12 B_a/MFR ratio versus weight average molecular weight \bar{M}_w of polymers studied

ing to a decrease in the recoverable elastic deformation and/or to an increase in the product flowability.

The discrepancies found in literature about the influence of *LCB* on the elastic properties of the polymers^{10,12,16,37,40} are partly due to the different methods adopted to evaluate the molecular parameters and partly to an incorrect comparison among samples with different molecular characteristics.

Tensile properties

Out of the several methods for the determination of the tensile properties of molten products⁴¹⁻⁴⁶, the melt tension tester runs best approach the practical conditions of use. Although, from the physical point of view, such a measurement can hardly be interpreted⁴⁷, as variable temperature and deformation ranges exist in the monofilament under stretch, it offers the advantage of extreme running simplicity and of supplying information, which may be related to the applicative behaviour of polymers, especially in industrial spinning and casting^{25,48,49}.

The results obtained, in terms of 'melt strength', *MS*, and breakage stretch ratio, *BSR*, determined at 180°C are shown in Table 4; the heterogeneity of the tensile behaviour of the samples under examination is noticed, even if some exhibit very close *MFR* values. The explanation must be looked for in the different molecular structures of the examined polyethylenes; Figures 13 and 14, respectively reporting the *MS* and *BSR* as a function of molecular weight, show the following dependences: by increasing the molecular weight \bar{M}_w , *MS* increases and *BSR* decreases; the increase in *LCB* causes a decrease in *MS* and an increase in *BSR*, the molecular weight being the same. The first remark is fairly obvious; the second is a consequence of the

decrease in melt viscosity by the effect of *LCB*, as already noticed for shear properties.

Figures 15 and 16 plot *MS* and *BSR* vs *MFR*; in this case *LCB* causes an increase in *MS* and a decrease in *BSR* the *MFR* being the same⁵⁰. Such behaviour does not disagree with Figures 13 and 14; in fact, while \bar{M}_w is an independent variable, *MFR* is a function of \bar{M}_w , of β and of the *LCB* content, hence *MFR* being the same, branched polyethylenes exhibit a higher molecular weight, corresponding to a higher tensile strength and to a lower breakage stretch ratio than those of the corresponding linear polymers. The fact that the behaviour of tensile parameters vs \bar{M}_w and *MFR* is of opposite sign means that the molecular weight exerts a pre-

Table 4 Tensile properties at 180°C measured by means of 'melt tension tester'

Sample No.	Melt strength (gr)	Breakage stretch ratio
1	2.45	79
2	3.1	52
3	5.2	21
4	1.6	263
5	1.7	253
6	0.43	2000
7	0.95	262
8	2.35	63
9	6.9	13
10	2.8	131
11	3.48	119
12	7.2	18
13	9.5	13
14	9.0	9
15	0.2	>2000
16	1.44	372
17	3.8	154
18	10.5	8

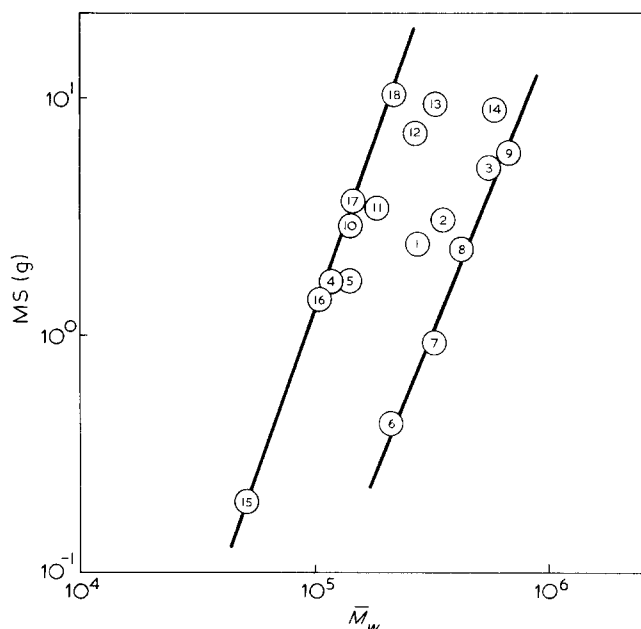


Figure 13 Melt strength *MS* at 180°C by MTT rheometer versus weight average molecular weight \bar{M}_w of samples used

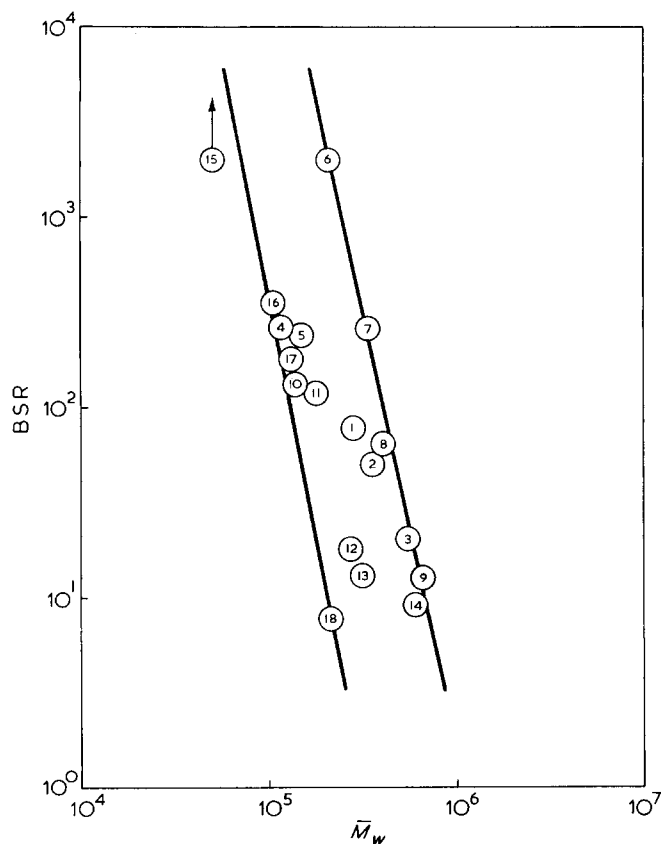


Figure 14 Breakage stretch ratio, *BSR*, at 180°C by MTT rheometer versus weight average molecular weight \bar{M}_w of samples examined

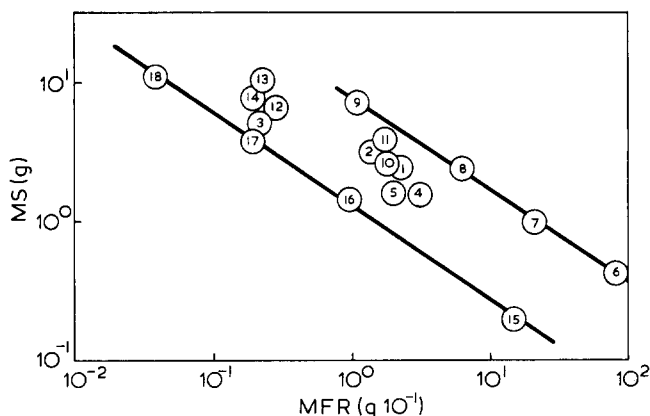


Figure 15 Melt strength, *MS*, at 180°C versus melt flow rate *MFR* of samples studied

dominant influence, in respect of *LCB*, on such properties of the melt. Figures 15 and 16, however, acquire considerable importance as technological maps; actually, by two simple measurements, such as the determination of tensile parameters by *MTT* and of *MFR*, it is possible to obtain a preliminary evaluation of the *LCB* content in polyethylene samples.

CONCLUSIONS

The rheological properties in the molten state of low-density polyethylenes are markedly different from those of the analogous high-density ones, mainly due to the presence of long branchings. In particular, in comparison with the linear

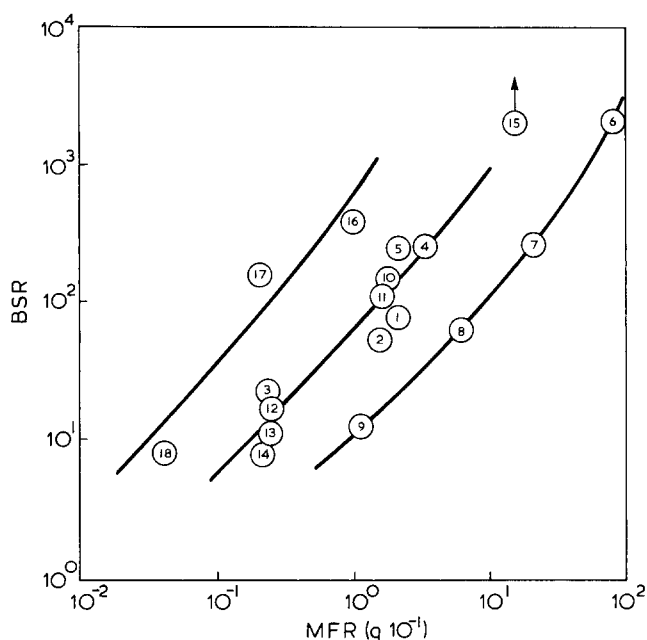


Figure 16 Breakage stretch ratio, *BSR*, at 180°C versus melt flow rate, *MFR*, of polyethylenes studied

polymers, the integral samples examined during the present investigation have shown that, the weight average molecular weight and the dimensional polydispersity being the same, the increase in *LCB* content involves the following variations of the rheological parameters:

- (i) the Newtonian viscosity undergoes a considerable decrease that may reach even three to four orders of magnitude;
- (ii) the limiting Newtonian shear rate is shifted toward higher values and follows a variation law that is inverse to the Newtonian viscosity;
- (iii) the limiting relaxation time of tangential stresses is lower and is substantially governed by the same parameters influencing η_0 ;
- (iv) the elastic deformation that may be recovered after extrusion is lower due to the more reduced size of branched macromolecules;
- (v) the melt strength considerably decreases and the breakage stretch ratio is consequently increased, in agreement with the melt viscosity decrease.

The results obtained prove that the above-discussed rheological parameters increase considerably with the molecular weight, except for the limiting Newtonian shear rate and for the breakage stretch ratio, which decrease.

As to the commercial LDPE products investigated here, the effect of molecular weight distribution on the rheological properties is negligible, compared with the very high effect exerted by the molecular weight and *LCB* content.

ACKNOWLEDGEMENTS

The authors would like to thank Prof. G. Pezzin for helpful suggestions and Mrs. B. Barboni and Mr. L. Ceron for their contribution.

REFERENCES

- 1 Tung, L. H. *J. Polym. Sci.* 1960, **46**, 409
- 2 Schreiber, H. P. *J. Appl. Polym. Sci.* 1965, **9**, 2101
- 3 Ram, A. and Narkis, M. *J. Appl. Polym. Sci.* 1966, **10**, 481

- 4 Saeda, S., Yotsuyanagi, J. and Yamaguchi, K. *J. Appl. Polym. Sci.* 1971, **15**, 277
- 5 Moore, L. D. *J. Polym. Sci.* 1959, **36**, 155
- 6 Schreiber, H. P. and Bagley, E. B. *J. Polym. Sci.* 1962, **58**, 29
- 7 Busse, W. F. and Langworth, R. *J. Polym. Sci.* 1962, **58**, 49
- 8 Ferguson, J., Wright, B. and Haward, R. N. *J. Appl. Chem.* 1964, **14**, 53
- 9 Guillet, J. E., Combs, R. L., Slonaker, D. F., Weemes, D. A. and Coover, H. W. *J. Appl. Polym. Sci.* 1965, **9**, 757
- 10 Combs, R. L., Slonaker, D. F. and Coover, H. W. *J. Appl. Polym. Sci.* 1969, **13**, 519
- 11 Mendelson, R. A., Bowles, W. A. and Finger, F. L. *J. Polym. Sci. (A-2)* 1970, **8**, 105
- 12 Mendelson, R. A. and Finger, F. L. *J. Appl. Polym. Sci.* 1973, **17**, 797
- 13 Chartoff, R. P. and Maxwell, B. *J. Polym. Sci. (A-2)* 1970, **8**, 455
- 14 Miltz, J. and Ram, A. *Polym. Eng. Sci.* 1973, **13**, 273
- 15 Kuhn, R., Kromer, H. and Rossmannith, G. *Angew. Makrom. Chem.* 1974, **40/41**, 361
- 16 Wild, L., Ranganath, R. and Knoblock, D. C. *Polym. Eng. Sci.* 1976, **16**, 811
- 17 Gianotti, G., Cicuta, A. and Romanini, D. *Polymer* (to be published)
- 18 Romanini, D. and Gianotti, G. Unpublished data
- 19 Desreux, V. and Bischoff, J. *Bull. Soc. Ch. Belg.* 1950, **59**, 93
- 20 Van Wazer, J. R., Lyons, J. W., Kim, K. Y. and Colwell, R. E. 'Viscosity and Flow Measurement' Interscience Publ. 1966
- 21 Bagley, E. B. *Trans. Soc. Rheol.* 1961, **5**, 355
- 22 Rabinowitsch, B. *Zeit. Physik. Chem.* 1929, **A145**, 1
- 23 Cox, W. P. and Merz, E. H. 'ASTM Special Technical Publ.' 1958, No 247
- 24 Pezzin, G. *Materie Plastiche* 1962, 1042
- 25 Hori, Y. and Hoshi, K. *Japan Plastics* 1969, Oct., 16
- 26 Romanini, D. unpublished data
- 27 Meissner, J. *J. Appl. Polym. Sci.* 1972, **16**, 2877
- 28 Romanini, D., Savadori, A. and Gianotti, G. to be published
- 29 Katoaka, T. and Ueda, S. *J. Appl. Polym. Sci.* 1968, **12**, 939
- 30 Graessley, W. W. *J. Chem. Phys.* 1967, **47**, 1942
- 31 Flory, P. J. 'Principles of Polymer Chemistry' Cornell Un. Press, London 1969
- 32 Middleman, S. 'The Flow of High Polymers' Interscience Publ. 1968
- 33 Ferry, J. D. 'Viscoelastic Properties of Polymers' J. Wiley Ed. 1970
- 34 Porter, R. S., Knox, J. P. and Johnson, J. F. *Trans. Soc. Rheol.* 1968, **12**: 3, 409
- 35 Blyler, L. L. *Rubber Chem. and Tech.* 1969, **42**, 823
- 36 Nakajima, N., Tirpak, G. A. and Shida, M. *Polym. Letters* 1965, **3**, 1089
- 37 Ram, A. *Polym. Eng. Sci.* 1977, **17**, 793
- 38 Rogers, M. G. *J. Appl. Polym. Sci.* 1970, **14**, 1679
- 39 Mendelson, R. A. and Finger, F. L. *J. Appl. Polym. Sci.* 1975, **19**, 1061
- 40 Han, C. D. and Villamizar, C. A. *J. Appl. Polym. Sci.* 1978, **22**, 1677
- 41 Meissner, J. *Rheol. Acta* 1971, **10**, 230
- 42 Cogswell, F. N. *Trans. Soc. Rheol.* 1972, **16**, 383
- 43 Meissner, J. *Trans. Soc. Rheol.* 1972, **16**, 405
- 44 Han, C. D. and Lamonte, R. R. *Trans. Soc. Rheol.* 1972, **16**, 447
- 45 Chen, I. J., Hagler, G. E., Abbott, L. E., Boguc, D. C. and White, J. L. *Trans. Soc. Rheol.* 1972, **16**, 473
- 46 Dealy, J. M. *Polym. Engin. Sci.* 1971, **11**, 433
- 47 Wissbrun, K. F. *Polym. Engin. Sci.* 1973, **13**, 342
- 48 Han, C. D. 'Rheology in Polymer Processing' Academic Press, London 1976
- 49 Kaltenbacher, E. J., Lund, J. K. and Mendelson, R. A. *SPF J.* 1967, Nov., 55
- 50 Busse, W. F. *J. Polym. Sci. (A-2)* 1967, **5**, 1249